Characterization of Physically Crosslinked Ionic Liquid-lignocellulose Hydrogels

Ionut Claudiu Roata, Catalin Croitoru,* Alexandru Pascu, and Elena Manuela Stanciu

A novel hydrogel was prepared starting with a 10-wt.% lignocellulose solution that was obtained by dissolution of Norway spruce wood (*Picea abies*) in the ionic liquid 1-butyl-3-methylimidazolium chloride. This ionic liquid was used to avoid traditional degradative and hazardous effects of solvents on the lignocellulose. Five alternate freezing and thawing cycles of the lignocellulose solution were employed as a means of physically crosslinking the hydrogels. The obtained hydrogel network was thermoreversible, with mesopores of 5 to 35 nm diameter, predominantly amorphous, and presenting distinct behaviors when immersed in aqueous solutions with different concentrations of organic electrolytes. The specific surface area of the hydrogel was 75.23 $m^2 \cdot g^{-1}$.The hydrogels presented high uptake capacities for pollutant chemical species (Cu^{2+}, Pb^{2+}, and bemacid blue anionic dye) that spanned from 445 mg/L to 547 mg/L at a pH value of 6. This indicated that the hydrogels are promising materials for environmental applications.

Keywords: Hydrogels; Lignocellulose; Crosslinking; Ionic liquids; Adsorption

*Contact information: Materials Engineering and Welding Department, Transilvania University of Braşov, Eroilor 29 Str, Braşov, 500036, Romania; *Corresponding author: c.croitoru@unitbv.ro*

INTRODUCTION

Hydrogels are a particular category of hydrophilic polymeric materials and are often employed in a plethora of environmental, pharmaceutical, and medical applications (Pasqui *et al.* 2012; Ahmed 2015). Polysaccharides, such as cellulose and its derivatives, starch, chitosan, alginates, derivatives of glycans, and others, are excellent candidates for use as hydrogel raw materials because of their excellent bioavailability, non-toxicity, low cost, ease of chemical functionalization, and hydrophilicity (Ji *et al.* 2017). Because of its high cellulose and hemicellulose contents, wood could be an efficient raw material for obtaining hydrogels. However, lignocelluloses are difficult to process with traditional solvents and often require the use of potentially toxic or corrosive solvent mixtures.

Ionic liquids (ILs), which is a class of milder environmentally-friendly organic compounds, have been employed in some studies as solvents for the dissolution of wood or its components (hemicelluloses and lignin). This has been done with the aim of obtaining hydrogels because of the well-known ability of ILs to disrupt the strong intermolecular bonding between polysaccharides and/or lignin macromolecules (Ibrahim *et al.* 2015; Song *et al.* 2016).

To avoid the destabilizing effect of a polar solvent on a macromolecular hydrogel network, various means of chemical stabilization (such as crosslinking with dicarboxylic acids, dialdehydes, and epichlorohydrin, and initiator-mediated grafting of unsaturated moieties) and physical stabilization (radiation crosslinking) have been employed to date (Ahmed 2015; Ciolacu *et al.* 2016). While having satisfactory efficiencies, these

crosslinking methods often pose potential detrimental environmental effects because of their inherent toxicity.

This paper aimed to obtain thermoreversible hydrogels from Norway spruce wood (*Picea abies*) lignocellulose dissolved in the IL 1-butyl-3-methylimidazolium chloride (BmimCl) through an environmentally friendly physical crosslinking method, namely alternate freezing and thawing cycles. This method has already been successfully applied to obtain poly (vinyl alcohol) [PVA]-based hydrogels (Hassan and Peppas 2000; Patachia *et al.* 2011). This method of crosslinking does not require the addition of potentially toxic crosslinkers into the system and removes the additional purification step required to remove unreacted traces of monomers, crosslinkers, solvents, and so forth.

There are already some reports in the reference literature dealing with the obtaining of PVA-hemicellulose composite hydrogels through the application of successive freezing-thawing cycles (Guan *et al.* 2014). However, to the knowledge of the authors, this method has not been applied before to obtain cellulose- or lignocellulose-derived gels starting from their corresponding solutions, without the addition of a gel-forming polymer or through changing the operational parameters of the system, such as its ionic strength or pH (Zhao *et al.* 2016). In addition, ionic liquid-containing hydrogels have not been obtained previously. The only reported "mild" physical crosslinking method for the purpose of obtaining hydrogels is that of (ligno)cellulose (Ciolacu *et al.* 2016) and other polysaccharides (Shen *et al.* 2016) precipitation from their solution by the solvent-exchange method. The crosslinking of the freeze-thawed hydrogel is thermoreversible and occurs through the formation of crystallites, which are highly ordered regions where cellulose/hemicellulose chains come into close contact and can interact strongly *via* hydrogen bonds.

A large variety of plant and bacteria-derived cellulosic materials (either in raw form or functionalized with anionic or cationic moieties) (Gao *et al.* 2018, Jamshaid *et al.* 2017), cellulose-polysaccharides/cellulose-synthetic polymer blends (Ma *et al.* 2017) or cellulose-based composite materials (Lessa *et al.* 2017), with a wide pore distribution (ranging from nanopores to macropores) have been widely applied in wastewater purification, due to their ease of processing, availability, and low cost. These biopolymeric systems present high affinity towards the adsorption of cationic and anionic dyes (Jamshaid *et al.* 2017) due to their polar (hydrophilic) groups and tunable specific surface area. Other mechanisms underlying (ligno)cellulose-derived materials application in wastewater remediation are represented by trapping/complexing (chelation) of heavy metal ions inside the pores or by ion exchange (Chandra *et al.* 2010).

The application potential of the obtained hydrogels in wastewater purification was studied using model solutions containing copper(II) ions (Cu^{2+}), lead(II) ions (Pb^{2+}), and bemacid blue (BB) dye, which is a high molecular mass anionic dye used in the textile industry for dying polyamide and wool articles.

EXPERIMENTAL

Materials

Norway spruce (*Picea abies*) wood flour (average diameter of 450 μm) was provided by the Wood Engineering Faculty of the Transilvania University of Braşov (Romania) and was dried at 105 °C before use.

The ILs used in this study, BmimCl and 1-hexyl-3-methylimidazolium chloride (HmimCl) with purities of 99.5%, were purchased from IoLiTec Ionic Liquids Technologies GmbH (Heilbronn, Germany). The BmimCl was freeze-dried for 24 h before use to remove water as much as possible.

The BB dye ($C_{31}H_{28}N_3NaO_6S$, M = 593.63 g/mol), copper(II) nitrate trihydrate ($Cu(NO_3)_2$), and lead(II) nitrate ($Pb(NO_3)_2$) had purities of 99.5% (Sigma-Aldrich, Taufkirchen, Germany).

Methods

The spruce wood lignocellulose solution in BmimCl (10 wt.% basis) was obtained by stirring the wood-IL mixture at 110 °C for 1 h until it was completely homogenized. The lignocellulose solution in BmimCl was poured into circular Petri dishes (30 mm diameter), sealed, and cooled to room temperature. The system was submitted to five alternate freezing-thawing cycles with the following parameters: freezing temperature of -50 °C, thawing temperature of room temperature (21 °C), and freezing and thawing durations of 24 h each. Five alternate freezing/thawing cycles were chosen because a lower number of cycles does not ensure the satisfactory stability of the gel for solvent action.

Cross-sectional scanning electron microscopy (SEM) micrographs of the gels were obtained with an A QUANTA 200 instrument (ThermoFisher Scientific, Hillsboro, Oregon, USA) at 1000x magnification. The collapsing of the hydrogel structure has been determined through image analysis of the SEM micrographs of the initial hydrogel and of the hydrogel in contact with water, using ImageJ software (assuming circular macropores shape), according to the procedure described elsewhere (Haeri and Haeri 2015). The software computes the macropores/voids diameter distribution, and through considering the values for the tails of the distribution in both cases, a relative decrease could be calculated.

The specific surface area (A_s, $m^2 \cdot g^{-1}$) of the hydrogel has been determined using the Brunauer–Emmett–Teller (BET) adsorption isotherm model and the pore size distribution of the material has been determined with the DFT method, by using a MicroMeritics TriStar 3000 instrument (Norcross, GA, U.S.A). These measurements were duplicated, and the differences in A_s and pore size distributions between parallel runs were found to be not more than 10%.

The crystallinity of the samples was assessed with X-ray diffraction (XRD) spectroscopy in the 2θ range of 5° to 60° (Bruker Advanced D8 Discover diffractometer, Ettlingen, Germany) with a scanning speed of 5°/min. The ATR-FTIR spectra of the lignocellulose hydrogel and starting materials were acquired with a Perkin Elmer BXII spectrometer (Rodgau, Germany) in the 4000 to 600 cm^{-1} interval, with 4 cm^{-1} resolution and 5 successive scans per spectrum.

The differential scanning calorimetry (DSC) thermograms were recorded with a Perkin Elmer Diamond instrument (Rodgau, Germany) (-60 °C to 40 °C, heating/cooling rate of 2 °C/min).

The swelling/collapsing ratio (w_t) of the gels (5-mm diameter samples) in distilled water and several electrolytes with 95 wt.%, 75 wt.%, and 25 wt.% BmimCl and HmimCl aqueous solutions were monitored by determining the sample mass at specific time intervals until an equilibrium was attained (25 °C),

$$w_t = \frac{m_t}{m_0} \quad (1)$$

where m_t is the mass of the gel at t minutes of water/solution immersion (g), and m_0 is the initial mass of the sample before immersion (g).

The uptake capacity of the hydrogel samples (initially equilibrated in water) for several model pollutants (heavy metal ions and organic dye) was determined by immersing them in stoppered glass vials with 10 mL of a solution at 25 °C and under 50-rpm magnetic stirring until equilibrium sorption was reached. Various initial concentrations in the $Cu(NO_3)_2$, $Pb(NO_3)_2$, and BB aqueous solutions (50 mg/L to 600 mg/L) were used. The concentration of the Cu^{2+} and Pb^{2+} was determined by flame atomic absorption spectrometry (FAAS; Analytic Jena, ZEEnit 700, Jena, Germany), and the concentration of the BB dye was determined by ultraviolet visible spectrophotometry (λ_{max} = 604 nm; Perkin-Elmer Lambda 25 spectrometer, Rodgau, Germany). The pH of all of the solutions was adjusted to 6 ± 0.2 with the addition of HNO_3 or NaOH solutions. Equation 2 was employed to assess the quantity of metal ions/dye adsorbed per 1 g of sorbent,

$$q_e = \frac{(c_0 - c_e) \cdot V}{m_s} \quad (2)$$

where q_e is the equilibrium adsorption capacity (mg/g), c_0 and c_e are the initial and adsorption equilibrium pollutant concentrations (mg/L), respectively, V is the volume of the solution (L), and m_s is the mass of the hydrogel sorbent sample (g).

All of the sorption studies were performed in triplicate to evaluate the reproducibility of the data.

RESULTS AND DISCUSSION

The SEM micrograph in Fig. 1a indicates that the freezing and subsequent thawing of the lignocellulose solution in BmimCl led to the production of an insoluble hydrogel having a web-like heterogeneous distribution of macropores (10 μm to 180 μm), of which form and size is dictated by the solvent (ionic liquid) crystallites, formed during freezing of the lignocellulose solution (Khan *et al.* 2016).

Because BmimCl is a good solvent for cellulose, the obtained hydrogel, containing BmimCl in composition was already in a "swollen state". Immersion in water determines the collapsing of the gel structure, as is indicated by the SEM micrograph in Fig. 1b. The average reduction in diameter of the macropores/voids after water immersion spanned from 20% to 70% compared with the original swollen hydrogel, as determined from the relative modification in the macropores size distributions related to the SEM micrographs from Fig. 1a and 1b. Furthermore, the region in contact with water (the top layer approximately 150 μm thick) had a granular appearance, which was caused by the precipitation of lignocellulose, and subsequently led to IL leakage from this area. This collapsed region created a diffusion barrier that has a dominating influence on the permeation rate of different chemical species into and from the gel, as well as on the sorption mechanism (da Silva Burgal *et al.* 2016). The presence of a diffusion barrier could prove useful in applications such as controlled delivery, separation of different compounds, and as an absorptive media (due to the high partition coefficient between the IL and water).

The obtained hydrogel was predominantly amorphous (crystallinity index of 21.1%), which was in contrast with the spruce wood starting material (crystallinity index of 38.2%). This is shown in the XRD diffractograms in Fig. 1c. In the XRD diffractogram of the lignocellulose hydrogel, the peaks corresponding to the cellulose I anomer (the (101) and the (040) diffraction planes) disappeared and left only the broad (002) contribution, which is characteristic of cellulose II (Croitoru *et al.* 2011a; Stanton *et al.* 2018). As previous research on poly(vinyl alcohol) cryogels has indicated (Hassan and Peppas 2000; Bajpai and Saini 2006), gelation may have been induced by the macromolecules being close to each other during the slow freezing of the lignocellulose solution in BmimCl, which led to the promotion of highly ordered regions where the polymer chains interact strongly *via* hydrogen bonding from the hydroxyl groups (Ricciardi *et al.* 2004). These ordered regions (crystallites) could remain intact during the following thawing cycle and act as crosslinking points in the network (Fig. 1d).

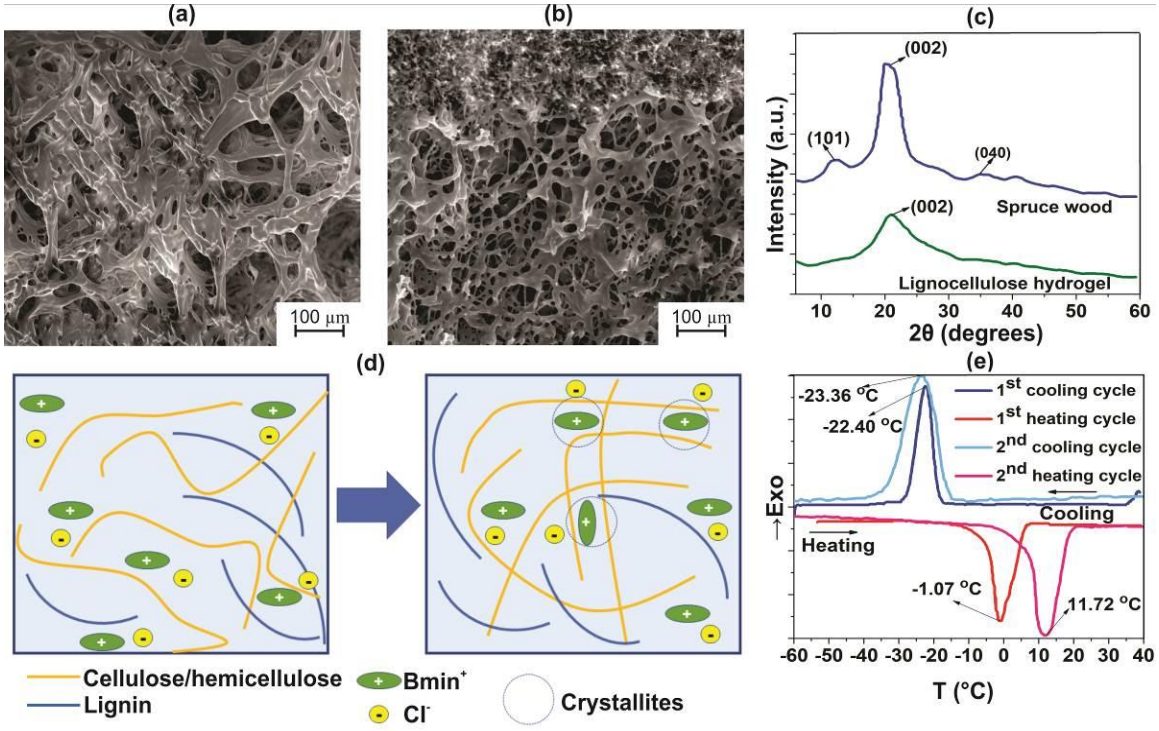

Fig. 1. SEM micrographs of the (a) neat lignocellulose hydrogel and (b) hydrogel after collapsing in water; (c) XRD diffractogram of the spruce wood and lignocellulose hydrogel; (d) gelation mechanism; and (e) DSC thermograms of the lignocellulose/IL solution

Figure 1e depicts the DSC thermograms for two successive cooling/heating cycles of the lignocellulose solution in BmimCl. While the melting point of pure BmimCl has been reported to be in the region of 76 °C to 78 °C (Nishikawa *et al.* 2007), the lignocellulose solution in BmimCl presented an exothermic crystallization peak centered at -22.40 °C (on the cooling curve of the first cycle), which was because of solute-solvent interactions.

Melting of the lignocellulose solution occurred at -1.07 °C (from the endothermic peak in the first cycle heating curve). Upon cooling the solution during the second cycle, a shifting of the crystallization peak to a lower temperature (-23.4 °C) and subsequent broadening was observed. The broadening in the case of the second cycle occurred because

of the presence of lignocellulose with a variable degree of crosslinking. It was seen that a shifting of the melting temperature to 11.7 °C occurred when heating the lignocellulose for the second time, which could have been an indication of physical crosslinking points in the system. The system was fully thermoreversible, which is useful when recycling of the IL is desired or in the case of sorbate recovery (*i.e.* when using the hydrogel as a sorption media).

The specific surface area of the hydrogel, as obtained from the BET isotherm model is 75.23 $m^2 \cdot g^{-1}$, comparable to that of other (ligno)celluloses (Aaltonen and Jauhiainen, 2009).

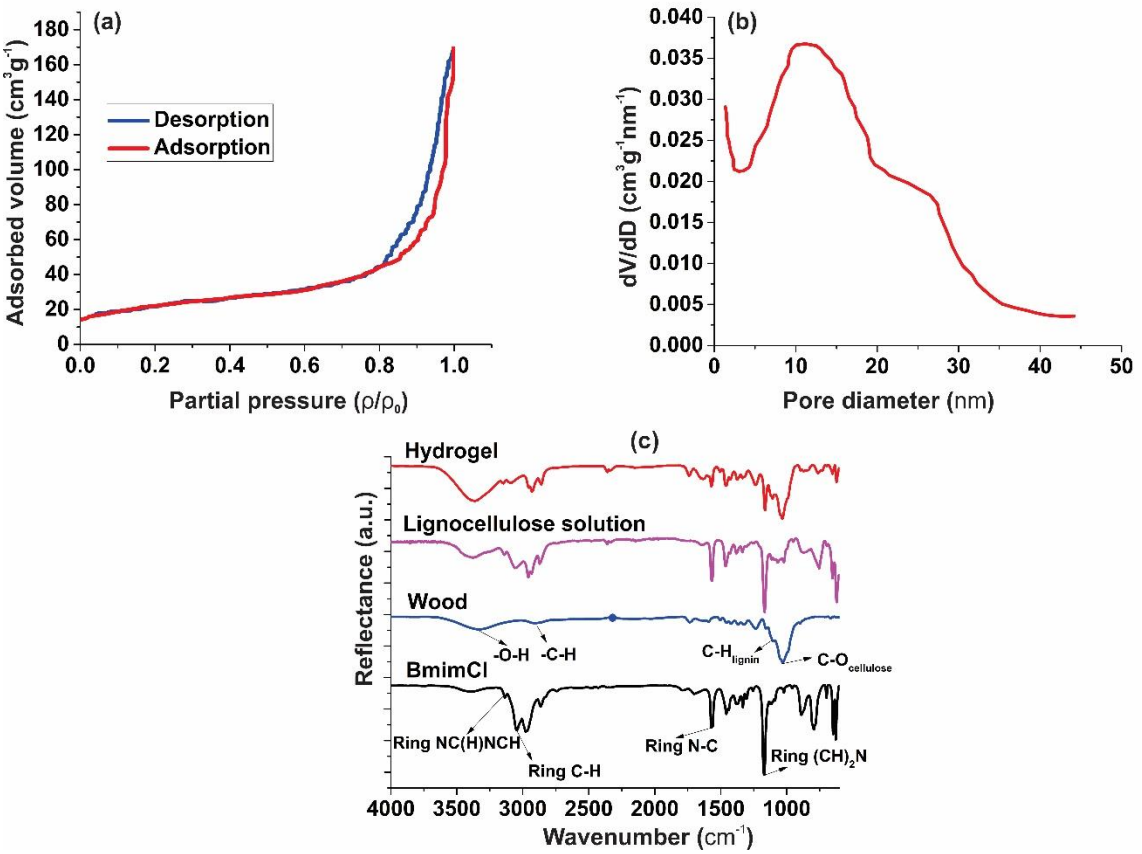

Fig. 2. (a) BET sorption-desorption isotherms for the hydrogel; (b) pore diameter distribution and (c) ATR-FTIR spectra of the hydrogel and starting materials

The N_2 adsorption-desorption isotherms are of type IV (Fig. 2a), with hysteresis loops of type H1 as classified by IUPAC, which are typical for mesoporous materials with slit-shaped pores (Sing 1985). The pore walls of the hydrogel are deformable, probably collapsing in the N_2 desorption step, generating the hysteresis loop from Fig. 2a, deducted through association with research on silica networks (Coasne *et al.* 2006). The pore size distribution also shows a mesoporous material, with the pore diameters spanning from 5 to 35 nm (Fig. 2b). It is to be noted that the BET isotherm does not apply to the macropores templated into the material by the IL crystallites and seen in the SEM micrographs (Veres *et al.* 2018).

The ATR-FTIR spectra (Fig. 2c) of BmimCl ionic liquid presents several intense bands, ascribed to -C-H stretching modes of imidazolium ring (3138 to 3057 cm^{-1}),

imidazolium -N-C- stretching vibration (1563 cm^{-1}), and imidazolic -CH_2 bending vibration (1169 cm^{-1}) (Croitoru *et al.* 2014; Moumene *et al.* 2015). The wood spectrum presents the usual absorption bands, characteristic of cellulose (broad -OH stretching vibration, ~3341 cm^{-1}, intense -C-O bending mode, ~1030 cm^{-1}, usually ascribed to cellulose crystallinity), lignin (aromatic -C-H in plane deformation, ~1115 cm^{-1}), respectively of all the wood components (cellulose, hemicellulose, lignin), namely the stretching vibration of -C-H groups, between 2970 and 2835 cm^{-1} (Popescu *et al.* 2007; Croitoru *et al.* 2011b). Only the vibrations that do not superimpose those of the IL were presented for wood. Through dissolution of the lignocellulose in the ionic liquid, the intensity of the -C-O band at ~1030 cm^{-1} is reduced in intensity with a factor of 5, indicating a destructuration of the crystalline cellulose network. The intensity of the -C-O band increases in the case of the hydrogel, in comparison with the starting lignocellulose solution, indicating a restructuration of the cellulose network. The red-shifting of this band at lower wavenumbers (~1025 cm^{-1}) may be an indicator of cellulose matrix flexibility, along with the converting of a significant amount of cellulose from the I anomer to the II anomer (Popescu *et al.* 2007; Croitoru *et al.* 2011a). An increase in the intensity of the -OH stretching vibration at ~3358 cm^{-1} in the hydrogel could imply mode -OH groups formation in cellulose, through oxidation during dissolution in BmimCl (beneficial for heavy metal ions and dyes adsorption), as well as a stiffening of the hydrogel matrix through the formation of more hydrogen bonds (blue shifting of the band maxima, comparing to wood).

Collapsing (syneresis) of the hydrogel network occurred during immersion in the distilled water (Fig. 3a), which was subsequently followed by the elimination of the IL from the material. This was confirmed by electrical conductance monitoring of the immersion water. The collapsing kinetics presented several pseudo-equilibria because of the two competing mass flow rates (IL exiting as water entered the crosslinked network) (Patachia *et al.* 2011). The first slow ongoing period in the w_t decrease may have correlated with the solutes crossing the "collapsed boundary" (boundary is shown in Fig. 3b). The same induction period related to the permeation of ILs from their aqueous solutions was also present in Figs. 3b and 3c. Because the two ILs (BmimCl and HmimCl) are good solvents for lignocellulose, swelling was expected to occur for the collapsed hydrogels (initially equilibrated in distilled water) immersed in the IL solutions, as it was determined in other research on chitosan hydrogels (Spinks *et al.* 2006). A higher swelling of the gel determines an improved mass flow of both water and IL inside the crosslinked network.

A lower induction time related to the permeation inside the collapsed hydrogel was recorded for the HmimCl (even if it had a higher molar mass than the BmimCl) because of its increased plasticizing effect on the cellulose, which determined the "softening" of the crosslinked network. For both the BmimCl and HmimCl aqueous solutions, multiple pseudo equilibria were recorded in the corresponding kinetics because of both the hindering effect of the lignin (which has a lower affinity for the ILs than cellulose or hemicellulose) and the distribution of the heterogeneous pores. Because of their high uptake ratios, these hydrogels could prove useful as sorption/concentration media to remove ILs from their aqueous solutions.

Good adsorption capacities were recorded for Cu^{2+} (542.8 mg/g), Pb^{2+} (475.3 mg/g), and the BB model anionic dye (446.0 mg/g) and were higher than has been reported in most research concerning biomass-derived gels (Zhou *et al.* 2012).

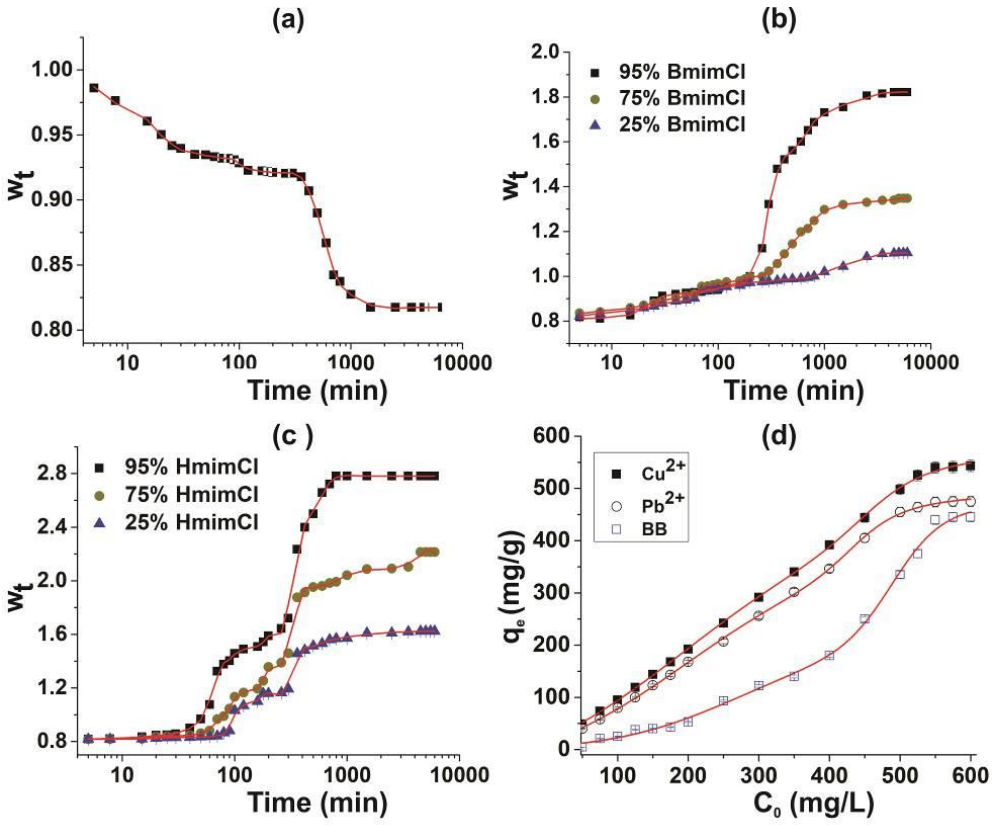

Fig. 3. (a) Hydrogel collapsing kinetics in distilled water; swelling kinetics in the (b) BmimCl solutions and (c) HmimCl solutions (log scale); and (d) adsorption isotherms for the Cu^{2+}, Pb^{2+}, and BB dye

The adsorption capacities reached equilibrium in the range of 500 mg/L to 600 mg/L. Two common adsorption models, Freundlich (Eq. 3) and Langmuir (Eq. 4) (Liu *et al.* 2018), were fitted to the experimental data on the adsorption of Cu^{2+}, Pb^{2+}, and the BB dye from the aqueous solutions (Fig. 3d). The results are given in Table 1,

$$\frac{c_e}{q_e} = \frac{1}{K_L \cdot q_{\max}} + \frac{c_e}{q_{\max}} \quad (3)$$

where c_e is the equilibrium concentration of the metal ions in the solution (mg/L), q_e is the adsorbed amount at equilibrium (mg/g), and K_L (L/mg) and q_{max} (mg/g) are Langmuir constants related to the energy of adsorption and maximum uptake per unit mass of the adsorbent, respectively.

$$q_e = K_F \cdot c_e^{1/n} \quad (4)$$

where K_F is the Freundlich constant corresponding to the adsorption capacity ((mg/g)·(mg/L)$^{1/n}$), and n represents a dimensionless heterogeneity factor for the adsorption sites.

The coefficients of determination (R^2) from Table 1 showed that the Freundlich isotherm model was able to fit the data in a more satisfactory manner as opposed to the Langmuir isotherm model (homogenous surface, monolayer adsorption), which was because the Freundlich isotherm model describes multilayer physical adsorption on media with heterogenous sorption sites (Kenawi *et al.* 2018). The affinity of the adsorbate for the

substrate was dictated by the K_F values, which indicated preferential sorption in the following order: $Cu^{2+} > Pb^{2+} >$ BB. The 1/n values were smaller than 1 for the heavy metal ions, which indicated a good affinity of the adsorbate for the substrate.

Table 1. Parameters for the Tested Adsorption Isotherm Models

Adsorbate	Freundlich Isotherm				Langmuir Isotherm		
	q_{max} (mg/g)	K_F (mg/g)·(L/mg)$^{1/n}$	1/*n*	R^2	q_{max} (mg/g)	K_L (L/mg)	R^2
Cu^{2+}	600.462	9.289	0.702	0.996	598.897	0.247	0.985
Pb^{2+}	654.172	8.062	0.781	0.994	600.154	0.166	0.987
BB	486.520	3.535	1.125	0.987	478.354	0.105	0.981

For BB, the 1/*n* value indicated a less favorable adsorption, which was probably because of the interaction of the bulky dye anion with the IL cations. The higher affinity of the heavy metal ions (Cu^{2+}, Pb^{2+}) for the cellulosic material could be due to their interaction with the -OH groups, respectively with the -C=O and -COOH groups of the partly oxidized cellulose II anomer which serve as active sites for metal binding in the hydrogel matrix (Jamshaid *et al.* 2017). On the other hand, the adsorption of the model anionic dye bemacid blue could be dictated by the higher partition coefficient of the dye in ionic liquid phase of the hydrogel, in contrast with water, as determined in other research (Pei *et al.* 2007).

CONCLUSIONS

1. Lignocellulose hydrogels were successfully obtained by an alternative physical crosslinking method of five alternate freezing-thawing cycles, using Norway spruce wood dissolved in BmimCl.
2. The gelation was thermoreversible and occurred *via* facilitating the interactions between several regions of the polysaccharide chains.
3. The hydrogels presented a heterogeneous distribution of macropores (10 μm to 180 μm) and mesopores (5 nm to 30 nm) and a modulated mass uptake response to different concentrations of aqueous electrolytes.
4. The hydrogels presented a good sorption capacity for Cu^{2+}, Pb^{2+}, and the BB anionic dye. It was found that the multilayer and heterogeneous sorption sites adsorption model characterized by the Freundlich isotherm was able to fit the experimental data in a satisfactory manner.

ACKNOWLEDGMENTS

This paper was supported by the Sectoral Operational Programme Human Resources Development (SOP HRD), which is financed by the European Social Fund and the Romanian Government under the contract number POSDRU/89/1.5/S/59323. The purchasing of the ILs was funded by the National University Council from Romania (CNCSIS) through the national grant IDEI 839/2008.

The authors acknowledge the structural funds project PRO-DD (POS-CCE, O.2.2.1., ID 123, SMIS 2637, ctr. No 11/2009) for providing the CDI Institute of Transilvania University of Braşov with the infrastructure that was used in this work. The help of Ph.D. Eng. Porzsolt Attila in performing the DSC analysis is acknowledged.

REFERENCES CITED

Aaltonen, O., and Jauhiainen, O. (2009). "The preparation of lignocellulosic aerogels from ionic liquid solutions," *Carbohydr. Polym.* 75, 125-129. DOI:10.1016/j.carbpol.2008.07.008.

Ahmed, E. M. (2015). "Hydrogel: Preparation, characterization, and applications: A review," *Journal of Advanced Research* 6(2), 105-121. DOI: 10.1016/j.jare.2013.07.006

Bajpai, A. K., and Saini, R. (2006). "Preparation and characterization of novel biocompatible cryogels of poly (vinyl alcohol) and egg-albumin and their water sorption study," *J. Mater. Sci.-Mater. M.* 17(1), 49-61. DOI: 10.1007/s10856-006-6329-z

Chandra, D., Das, S. K., and Bhaumik, A. (2010). "A fluorophore grafted 2D-hexagonal mesoporous organosilica: Excellent ion-exchanger for the removal of heavy metal ions from wastewater," *Microporous Mesoporous Mater*. 128, 34-40. DOI:10.1016/j.micromeso.2009.07.024.

Ciolacu, D., Rudaz, C., Vasilescu, M., and Budtova, T. (2016). "Physically and chemically cross-linked cellulose cryogels: Structure, properties and application for controlled release," *Carbohyd. Polym.* 151, 392-400. DOI: 10.1016/j.carbpol.2016.05.084

Croitoru, C., Patachia, S., Porzsolt, A., and Friedrich, C. (2011a). "Effect of alkylimidazolium based ionic liquids on the structure of UV-irradiated cellulose," *Cellulose* 18(6), 1469-1479. DOI: 10.1007/s10570-011-9586-z

Croitoru, C., Patachia, S., Porzsolt, A., and Friedrich, C. (2011b). "Ecologic modification of wood using alkylimidazolium-based ionic liquids," *Environ. Eng. Manag. J.* 10 (8), 1149-1154.

Croitoru, C., Patachia, S., Doroftei, F., Parparita, E., and Vasile, C. (2014). "Ionic liquids influence on the surface properties of electron beam irradiated wood," *Appl. Surf. Sci*. 314, 956-966. DOI:10.1016/j.apsusc.2014.06.142.

Coasne, B., Galarneau, A., Di Renzo, F., and Pellenq, R. J. M. (2006). "Gas adsorption in mesoporous micelle-templated silicas: MCM-41, MCM-48, and SBA-15," *Langmuir*. 22(26), 11097-11105. DOI:10.1021/la061728h.

da Silva Burgal, J., Peeva, L., and Livingston, A. (2016). "Towards improved membrane production: Using low-toxicity solvents for the preparation of PEEK nanofiltration membranes," *Green Chem.* 18(8), 2374-2384. DOI: 10.1039/C5GC02546J

Gao, X., Zhang H., Chen, K., Zhou, J., and Liu, Q. (2018). "Removal of heavy metal and sulfate ions by cellulose derivative-based biosorbents," *Cellulose* 25, 2531-2545. DOI:10.1007/s10570-018-1690-x.

Guan, Y., Bian, J., Peng, F., Zhang, X.-M., and Sun, R.-C. (2014). "High strength of hemicelluloses based hydrogels by freeze/thaw technique," *Carbohyd. Polym*. 101, 272-280. DOI: 10.1016/j.carbpol.2013.08.085

Haeri, M., and Haeri, M. (2015). "ImageJ plugin for analysis of porous scaffolds used in tissue engineering," *Journal of Open Research Software* 3:e1. DOI: 10.5334/jors.bn.

Hassan, C. M., and Peppas, N. A. (2000). "Structure and morphology of freeze/thawed PVA hydrogels," *Macromolecules* 33(7), 2472-2479. DOI: 10.1021/ma9907587

Ibrahim, M. M., Abd-Eladl, M., and Abou-Baker, N. (2015). "Lignocellulosic biomass for the preparation of cellulose-based hydrogel and its use for optimizing water resources in agriculture," *J. Appl. Polym. Sci.* 132(42). DOI: 10.1002/app.42652

Jamshaid, A., Hamid, A., Muhammad, N., Naseer, A., Ghauri, M., Iqbal, J., Rafiq, S., and Shah, N.S. (2017). "Cellulose-based Materials for the Removal of Heavy Metals from Wastewater - An Overview," *ChemBioEng Rev.* 4, 240-256. DOI:10.1002/cben.201700002.

Ji, X., Zhang, Z., Chen, J., Yang, G., Chen, H., and Lucia, L. A. (2017). "Synthesis and characterization of alkali lignin-based hydrogels from ionic liquids," *BioResources* 12(3), 5395-5406. DOI: 10.15376/biores.12.3.5395-5406

Kenawi, I. M., Hafez, M. A. H., Ismail, M. A., and Hashem, M. A. (2018). "Adsorption of Cu(II), Cd(II), Hg(II), Pb(II) and Zn(II) from aqueous single metal solutions by guanyl-modified cellulose," *Int. J. Biol. Macromol.* 107(Pt B), 1538-1549. DOI: 10.1016/j.ijbiomac.2017.10.017

Khan, M. J., Zhang, J., and Guo, Q. (2016). "Covalent/crystallite cross-linked co-network hydrogels: An efficient and simple strategy for mechanically strong and tough hydrogels," *Chem. Eng. J.* 301, 92-102. DOI:10.1016/j.cej.2016.04.025.

Lessa, E. F., Medina, A. L., Ribeiro, A. S., and Fajardo, A. R. (2017). "Removal of multi-metals from water using reusable pectin/cellulose microfibers composite beads," *Arab. J. Chem*. DOI:10.1016/j.arabjc.2017.07.011.

Liu, C., Omer, A. M., and Ouyang, X.-K. (2018). "Adsorptive removal of cationic methylene blue dye using carboxymethyl cellulose/k-carrageenan/activated montmorillonite composite beads: Isotherm and kinetic studies," *Int. J. Biol. Macromol.* 106, 823-833. DOI: 10.1016/j.ijbiomac.2017.08.084

Ma, J., Zhou, G., Chu, L., Liu, Y., Liu, C., Luo, S., and Wei, Y. (2017). "Efficient removal of heavy metal ions with an EDTA functionalized chitosan/polyacrylamide double network hydrogel," *ACS Sustain. Chem. Eng*. 5, 843-851. DOI:10.1021/acssuschemeng.6b02181

Moumene, T., Belarbi, E.H., Haddad, B., Villemin, D., Abbas, O., Khelifa, B., and Bresson, S. (2015) "Study of imidazolium dicationic ionic liquids by Raman and FTIR spectroscopies: The effect of the nature of the anion," *J. Mol. Struct.* 1083, 179-186. DOI:10.1016/j.molstruc.2014.11.061.

Nishikawa, K., Wang, S., Katayanagi, H., Hayashi, S., Hamaguchi, H.-o., Koga, Y., and Tozaki, K.-i. (2007). "Melting and freezing behaviors of prototype ionic liquids, 1-butyl-3-methylimidazolium bromide and its chloride, studied by using a nano-watt differential scanning calorimeter," *J. Phys. Chem. B* 111(18), 4894-4900. DOI: 10.1021/jp0671852

Pasqui, D., De Cagna, M., and Barbucci, R. (2012). "Polysaccharide-based hydrogels: The key role of water in affecting mechanical properties," *Polymers-Basel* 4(3), 1517-1534. DOI: 10.3390/polym4031517

Patachia, S., Friedrich, C., Florea, C., and Croitoru, C. (2011). "Study of the PVA hydrogel behavior in 1-butyl-3-methylimidazolium tetrafluoroborate ionic liquid," *Express Polym. Lett.* 5(2), 197-207. DOI: 10.3144/expresspolymlett.2011.18

Popescu, C. M., Popescu, M. C., Singurel, G., Vasile, C., Argyropoulos, D. S., and Willfor, S. (2007). "Spectral characterization of eucalyptus wood," *Appl. Spectrosc*. 61(11). 1168-1177. DOI:10.1366/000370207782597076.

Pei, Y. C., Wang, J. J., Xuan, X. P., Fan, J., and Fan, M. (2007). "Factors affecting ionic liquids based removal of anionic dyes from water," *Environ. Sci. Technol*. 41, 5090-5095. DOI:10.1021/es062838d.

Ricciardi, R., Auriemma, F., Gaillet, C., De Rosa, C., and Lauprêtre, F. (2004). "Investigation of the crystallinity of freeze/thaw poly(vinyl alcohol) hydrogels by different techniques," *Macromolecules* 37(25), 9510-9516. DOI: 10.1021/ma048418v

Shen, X., Shamshina, J. L., Berton, P., Bandomir, J., Wang, H., Gurau, G., and Rogers, R. D. (2016). "Comparison of hydrogels prepared with ionic-liquid-isolated *vs.* commercial chitin and cellulose," *ACS Sustain. Chem. Eng.* 4(2), 471-480. DOI:10.1021/acssuschemeng.5b01400.

Sing, K. S. W. (1985). "Reporting physisorption data for gas/solid systems with special reference to the determination of surface area and porosity," *Pure Appl. Chem.* 5. DOI:10.1351/pac198557040603.

Song, X., Chen, F., and Liu, S. (2016). "A lignin-containing hemicellulose-based hydrogel and its adsorption behavior," *BioResources* 11(3), 6378-6392. DOI: 10.15376/biores.11.3.6378-6392

Spinks, G. M., Lee, C. K., Wallace, G. G., Kim, S. I., and Kim, S. J. (2006). "Swelling behavior of chitosan hydrogels in ionic liquid-water binary systems," *Langmuir* 22(22), 9375-9379. DOI:10.1021/la061586r

Stanton, J., Xue, Y., Pandher, P., Malek, L., Brown, T., Hu, X., and Salas-de la Cruz, D. (2018). "Impact of ionic liquid type on the structure, morphology and properties of silk-cellulose biocomposite materials," *Int. J. Biol. Macromol.* 108, 333-341. DOI: 10.1016/j.ijbiomac.2017.11.137

Veres, P., Sebők, D., Dékány, I., Gurikov, P., Smirnova, I., Fábián, I., and Kalmár, J. (2018). "A redox strategy to tailor the release properties of Fe(III)-alginate aerogels for oral drug delivery," *Carbohydr. Polym.* 188, 159-167. DOI:10.1016/j.carbpol.2018.01.098.

Zhao, Y., Shen, W., Chen, Z., and Wu, T. (2016). "Freeze-thaw induced gelation of alginates," *Carbohyd. Polym.* 148, 45-51. DOI: 10.1016/j.carbpol.2016.04.047

Zhou, Y., Zhang, L., Fu, S., Zheng, L., and Zhan, H. (2012). "Adsorption behavior of Cd^{2+}, Pb^{2+}, and Ni^{2+} from aqueous solutions on cellulose-based hydrogels," *BioRes*ources 7(3), 2752-2765. DOI: 10.15376/biores.7.3.2752-2765

Article submitted: March 24, 2018; Peer review completed: May 24, 2018; Revised version received: June 7, 2018; Accepted: June 10, 2018; Published: June 21, 2018.
DOI: 10.15376/biores.13.3.6110-6121